Applications of OBC recording

Brian H. Hoffe and Laurence R. Lines, University of Calgary
Peter W. Cary, Sensor Geophysical, Calgary, Alberta, Canada

In recent years, there has been much interest in seismic imaging within the marine environment via four-component (4-C) ocean-bottom-cable (OBC) recording. The 4-C OBC sensor is equipped with a single hydrophone (pressure detector) plus a three-component (3-C) geophone (particle velocity detector). The 3-C geophone records the full three-dimensional ground motion via one vertical component and two orthogonal horizontal components. 4-C OBC recording has several advantages over conventional towed-streamer technology, including:

1) dual-sensor summation (hydrophone + vertical geophone signals) for the suppression of receiver-side multiples
2) utilizing *P-S* wave conversions for enhanced imaging
3) attenuation of free-surface multiples when combined with towed-streamer recordings

This article explores many of these elastic-wave imaging possibilities from a simple mathematical viewpoint and presents synthetic and real data examples for these applications.

Marine seismic wavefields. Figure 1 shows the simplest situation—a hydrophone and a geophone at the ocean bottom and vertical raypaths through the water column. We use the following notation from Paffenholz and Barr (1995): P = wavefield pressure; V = velocity of displacement; U = upgoing wavefield; D = downgoing wavefield; ρ = density of water; c = acoustic wave velocity of water.

By using the one-dimensional wave equation, Loewenthal et al. (1985) show that pressure waves are given by:

$$P = U + D \tag{1}$$

and the velocity of displacement wavefield is given by:

$$V = \frac{1}{\rho c}(U - D) \tag{2}$$

Pressure, a scalar quantity, is independent of the U or D directions. Total wavefield pressure is the sum of pressure from the upgoing and downgoing wavefields. A hydrophone is a recording device (usually piezoelectric) which measures wavefield pressure. It is insensitive to the wave's direction and therefore detects no difference between an upgoing compression and a downgoing compression.

Velocity of displacement is a vector quantity and therefore is influenced by wave direction. A geophone measures the velocity of a wave's displacement and detects a difference in sign between an upgoing compression and a downgoing compression. The sign convention is somewhat arbitrary and depends on the definition of the coordinate system. Like the rule of driving on the left or right side of the road, the sign convention is arbitrary but important to know. For the purposes of this discussion, we will choose the downward-traveling compression as positive, and we will multiply V by the scalar constant ρc so as to use $V = U - D$ in subsequent discussions.

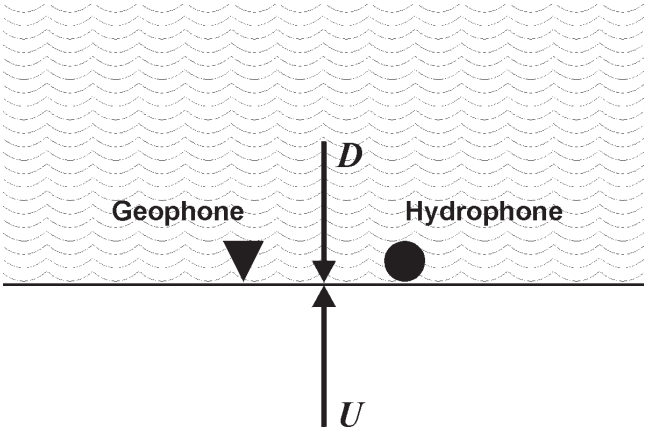

Figure 1. Hydrophone and geophone at the ocean bottom record the vertically traveling upgoing (*U*) and downgoing (*D*) wavefields.

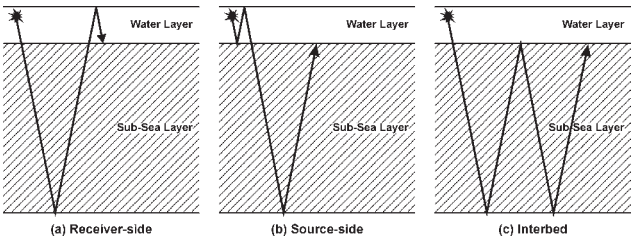

Figure 2. Multiple nomenclature in this paper: (a) receiver-side multiples, (b) source-side multiples, and (c) interbed multiples. Receiver-side multiples would consist of downgoing energy; both source-side and interbed multiples consist of upgoing energy.

Use of dual sensors for multiple suppression. Combining hydrophones and geophones at the ocean bottom essentially means using a "dual-sensor." The combined hydrophone or pressure recording (P) and the vertical geophone or displacement velocity recording (V) allows us to suppress receiver-side multiples. For the purpose of clarity, Figure 2 illustrates the multiple nomenclature used in this paper. The concept of dual-sensors has been explored by Loewenthal et al. (1985), Barr and Sanders (1989), Dragoset and Barr (1994), and Paffenholz and Barr (1995) among others. These analyses usually assume vertical wave propagation through the water column but sometimes allow nonvertical propagation above an acoustic seafloor. A theoretically complete analysis of water-layer multiple attenuation with 4-C receivers (hydrophone + 3-C geophone) on an elastic seafloor, which includes the dual-sensor situation considered here, has been presented by Osen et al. (1999).

Figure 3 depicts a wavefield trapped in a water layer with a surface reflection coefficient of –1 for reflected pressure waves impinging upon this free surface from below, and a reflection coefficient of R for pressure waves reaching the ocean bottom from above. We consider the downgoing and upgoing waves at the ocean bottom for a water layer with two-way traveltime τ and we consider the ini-

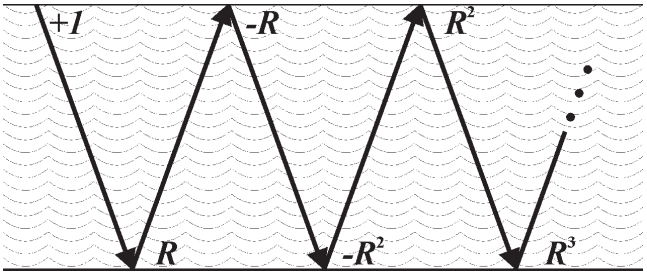

Figure 3. Reverberatory sequence for water-trapped seismic arrivals. Note the alternating sign and diminishing amplitudes ($R < 1$).

tial downgoing compressional wavefield to be initiated at time $t = -\tau/2$ so that $t = 0$ occurs when the first arrival impinges on the ocean bottom with amplitude +1. Upon arrival at the ocean bottom, the wave is partially reflected upward as a compression with amplitude R. It travels upward for time $\tau/2$ before being reflected downward from the ocean surface as a rarefraction with amplitude –R, arriving at the ocean bottom at time t where it is again reflected upward as a rarefraction with amplitude $-R^2$. These water-trapped arrivals continue as a series of reflections with diminishing amplitudes and alternating signs. If Z is the delay operator for two-way travel through the water layer, we can consider z transforms for the downgoing and upgoing waves.

At the ocean bottom, the downgoing wave's z transform is:

$$D(Z) = 1 - RZ + R^2Z^2 + ... = \frac{1}{(1 + RZ)} \qquad (3)$$

and the upgoing wave's z transform is:

$$U(Z) = R - R^2Z + R^3Z^3 + ... = \frac{R}{(1 + RZ)} \qquad (4)$$

The z transform for the pressure wavefield, as recorded by the hydrophone, is:

$$P(Z) = \frac{(1 + R)}{(1 + RZ)} \qquad (5)$$

The z transform for the velocity of displacement wavefield, as recorded by the geophone, (to within scalar multiplier ρc) is $V(Z) = U(Z) - D(Z)$ or:

$$V(Z) = \frac{R\text{-}1}{1+RZ} \qquad (6)$$

By inspection of equations (5) and (6), we see that:

$$P(Z) + \frac{(1 + R)}{(1 - R)}[V(Z)] = 0 \qquad (7)$$

In other words, a summation of the hydrophone recording which measures pressure with a scaled version of the vertical geophone recording which measures velocity of displacement removes one type of multiple. The dual-sensor combination of the hydrophone and vertical geophone recordings will cancel out all receiver-side multiples, while preserving reflections from below the ocean-bottom interface.

This is illustrated in Figure 4 where the upgoing reflectivity's z transform $\beta = \sum R_n z^n$. (Note the use of lower case z in the z transform because the delay operator for the time-

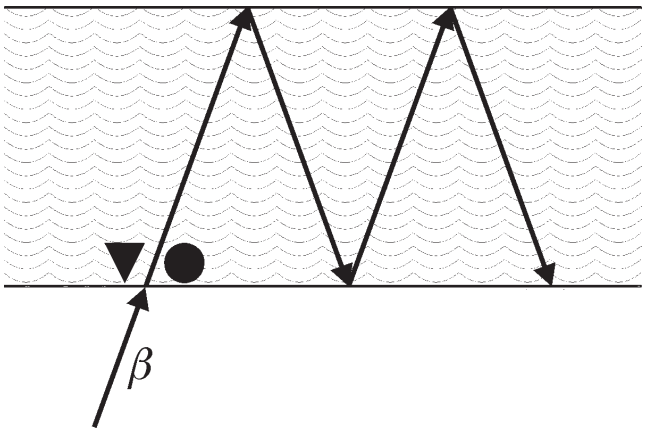

Figure 4. Upgoing reflectivity, β, and subsequent receiver-side multiples.

sampled reflectivity will generally not coincide with the delay operator for the multiples, i.e. $Z = z^r$). We can consider the upgoing wavefield, β, to be filtered by the multiples so that the z transform for the upgoing wavefield at the ocean bottom, as shown in Figure 4, is:

$$U(Z) = (1 - RZ + R^2Z^2 + ...)\beta = \frac{\beta}{(1 + RZ)} \qquad (8)$$

and the downgoing wavefield is:

$$D(Z) = (-Z + RZ^2 - R^2Z + ...)\beta = \frac{-Z\beta}{(1 + RZ)} \qquad (9)$$

so that

$$P(Z) = \frac{(1 - Z)}{(1 + RZ)}\beta \qquad (10)$$

and

$$V(Z) = \frac{(1 + Z)}{(1 + RZ)}\beta \qquad (11)$$

Adding these wavefields as before in equation (7), we obtain:

$$P(Z) + \frac{(1 + R)}{(1 - R)}V(Z) = \frac{2}{(1 - R)}\beta \qquad (12)$$

Therefore, adding a hydrophone and scaled vertical geophone measurement leaves the reflectivity intact (except for a constant factor) while canceling out the receiver-side multiples. Source-side multiples still remain in the data. Notice that addition of the hydrophone and geophone without any scaling cancels out the receiver ghost and leaves both receiver-side and source-side multiples, so the OBC data can be converted to ordinary streamer data in this fashion. With either strategy, the multiples that remain after the dual-sensor data have been combined generally need to be attacked by a more traditional multiple attenuation technique.

Synthetic example. Figure 5 compares synthetic seismograms computed for the hydrophone, scaled vertical geophone, and their dual-sensor summed result. These seismograms were computed from a general elastic wave model obtained by using *P*-wave and *S*-wave sonic logs from the Jeanne d'Arc Basin, offshore Newfoundland. The hydrophone and scaled vertical geophone data show a

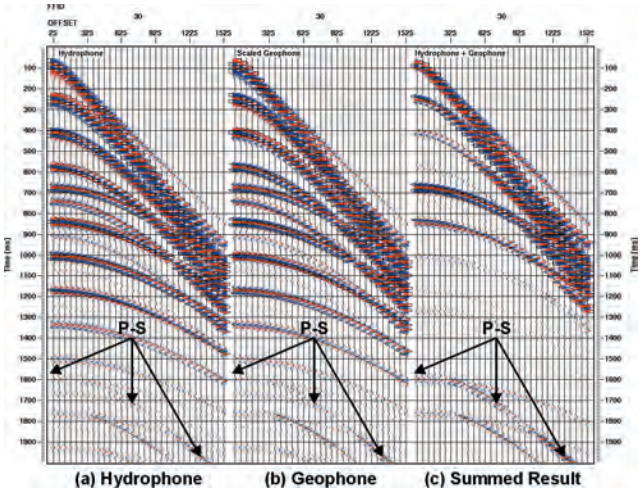

Figure 5. Synthetic OBC seismic data computed from a general elastic-wave model of the Jeanne d'Arc Basin for offsets 25-1525 m. (a) Hydrophone source gather, (b) scaled geophone source gather, and (c) dual-sensor summation result. Note on (c) that receiver-side multiples are greatly reduced in amplitude. Note also that (a), (b), and (c) show strong, mode-leaked, converted-wave arrivals (labeled "*P-S*") from the top of the second subsea layer.

large number of various water-layer multiples at 600-1600 ms, but they are greatly reduced on the summed result. Note the *P-S* converted arrivals on all three seismograms. Images of these converted-wave arrivals prove useful in marine seismic imaging, as we will see in the next section.

It is important to reiterate that the dual-sensor method can directly remove only receiver-side multiples (i.e. downgoing multiples) and not other types of water-layer multiples. Although Equation (12) clearly demonstrates that the summation leaves the upgoing reflectivity intact, this reflectivity is usually contaminated by both source-side and interbed multiples (i.e., upgoing multiples).

This limitation of the dual-sensor method can be examined from a more physical viewpoint. Figure 6 displays a zoomed portion of the dual-sensor summed seismogram of Figure 5c between 600 and 2200 ms. Although the receiver-side multiples are greatly reduced in amplitude, a number of other water-layer multiples are not. These are identified on the seismogram by their corresponding raypath schematic.

Elaborating further on our sign conventions, we chose the hydrophone to measure a compression as positive and rarefraction as negative. We chose the vertical geophone to measure a downgoing compression as positive, downgoing rarefraction as negative, upgoing compression as negative, and upgoing rarefraction as positive. As Figure 6 indicates, because the upgoing reflectivity is contaminated by either source-side multiples, interbed multiples, or a combination of both, the hydrophone and vertical geophone will record this upgoing multiple energy with the same sign (i.e., hydrophone compression = geophone upgoing compression = negative; hydrophone rarefaction = geophone upgoing rarefaction = positive). Thus, upon summation of the hydrophone and scaled vertical geophone signals, these multiple types will constructively add. This is why there is residual multiple energy after summation.

Real data example. A real data example of dual-sensor

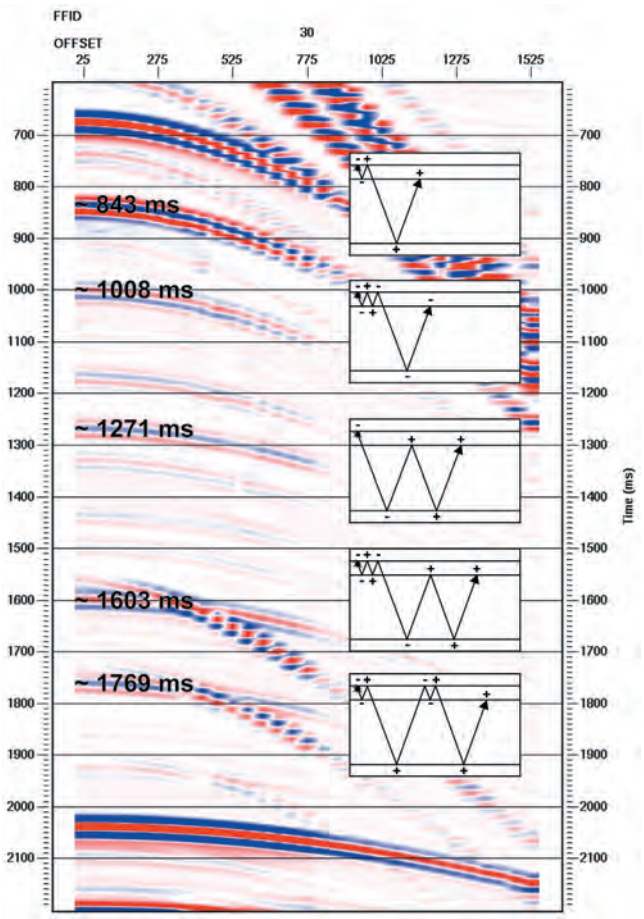

Figure 6. Zoomed portion of Figure 5c showing various water-layer multiples (and corresponding raypath schematic) that have not been suppressed by dual-sensor summation. These other multiple types are source-side, interbed, or a combination (i.e,. upgoing multiple energy).

combination is provided by the hydrophone and vertical geophone components of a 4-C OBC survey acquired by Geco-Prakla over the Mahogany Field, Gulf of Mexico (Caldwell et al., 1998). Figure 7 shows a portion of a receiver gather from this survey. Prominent primary events are visible on both the hydrophone traces and the geophone traces at near-offset arrival times of about 1190 ms and 1690 ms. Water depth is about 120 m, so the ghost, the first receiver-side, and source-side multiples all arrive about 160 ms after each primary event. The second multiple event is also visible about 160 ms later. Notice that the primaries are in phase and the multiples are out of phase on the two components. Also notice that the amplitude of the first multiple on the hydrophone component is actually higher than the amplitude of the primary, which is in accordance with theory when the seafloor reflection coefficient is positive (about 0.4 in this case). The summed result shows considerable reduction in the amplitude of the multiples compared to the primaries. However, source-side multiple energy remains, as expected.

Using converted waves to enchance imaging. Recent case histories from some North Sea fields have documented improved seismic imaging through gas-filled sediments using marine converted-wave data with startling results. An excellent example of this is provided by Granli et al. (1999).

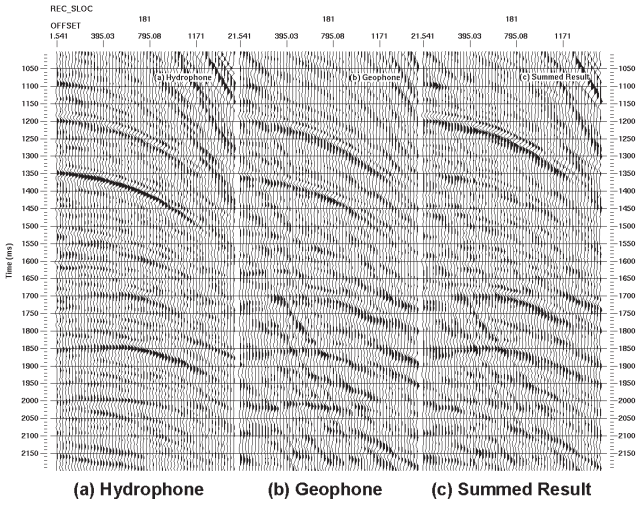

Figure 7. OBC seismic data acquired from Mahogany Field, Gulf of Mexico: (a) hydrophone data, (b) geophone data, and (c) summed result. Note the considerable reduction in amplitude of multiples compared to primaries between 1190 and 1690 ms.

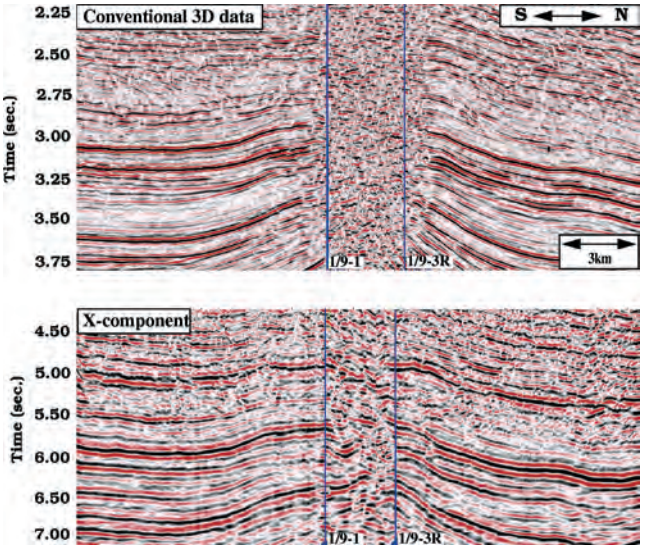

Figure 8. Comparison of *P-P* CMP (top) stack from 3-D streamer data and *P-S* CCP (bottom) stack from OBC data for Tommeliten Field. Note how the *P-S* stack produces a much better image in the presence of gas than the *P-P* image (from Granli et al.).

The Tommeliten chalk fields in the southern North Sea have substantial gas chimneys (~2 km wide) associated with them. These chimneys are caused by updip leakage of gas along faults that extend from the reservoir level into the overlying sediments. The presence of these gas-charged sediments severely distorted the *P*-wave seismic image obtained from previous conventional 3-D streamer surveys. White (1975) demonstrated that the presence of gas in the subsurface has a strong effect on *P*-waves. The reason for this, as Granli et al. point out, is that the bulk modulus, defined as the degree to which a rock is resistant to compression, is a key constituent in the definition of *P*-wave velocity (i.e. $V_p = \sqrt{[k + (4/3)\mu]/\rho}$ where k, μ, and ρ are respectively the bulk modulus, shear modulus, and density) and is severely distorted in the presence of gas. Small amounts of gas will seriously affect both the traveltime and reflection amplitude for *P*-waves and, unfortunately, processing of these data can only marginally compensate for this effect.

To resolve this imaging problem at the Tommeliten fields, Granli et al. turned to marine multicomponent OBC recordings to image the reservoir using converted or *P-S* data. The presence of gas usually has a small effect on the rock density and no significant effect on its shear modulus. The shear modulus is generally defined as the degree to which a rock is resistant to deformation and is the key constituent in the definition of the *S*-wave velocity (i.e., $V_s = \sqrt{\mu/\rho}$. Thus, *S*-waves produced via mode-conversion are much less affected by the presence of gas than *P*-waves.

Figure 8 compares a migrated *P-S* CCP (common conversion point) stack with a *P-P* CMP (common midpoint) stack from Tommeliten Field. The CCP stack was produced from newly acquired OBC converted-wave data and the CMP stack was produced from previously acquired conventional 3-D streamer *P*-wave data. As Granli et al. demonstrate and which is clearly evident from Figure 8, converted waves can be used to successfully image through a gas chimney. Also, they point out that the most important mode conversion in the marine multicomponent data from Tommeliten Field is conversion from *P* to *S* at the reservoir level.

Another excellent case history, also from the North Sea, documenting enhanced seismic imaging using converted waves when there is poor *P-P* reflectivity is by MacLeod et al. (1999).

The producing reservoir in Alba Field in the central North Sea is a poorly consolidated Eocene turbidite channel sand that can be up to 100-m thick. Its average subsea depth is 2000 m. This channel contains intrareservoir shales that can cause significant drilling and production problems as the oil production comes from several horizontally drilled wells.

Because it was critical that the horizontal wells be placed as close to the top of the reservoir as possible, accurate maps were required of the reservoir top and the intrareservoir shales. This mapping was extremely difficult with the existing streamer data because the reservoir top is a weak and inconsistent seismic event and the intrareservoir shales are often seismically invisible.

The shale-oil interface is extremely difficult to map using conventional *P*-wave streamer data because the oil sands and shales have, on average, the same acoustic impedance. A dipole sonic log acquired through the reservoir showed a significant *S*-wave impedance contrast at both the top and bottom of the reservoir. Subsequent seismic modeling using this dipole sonic information showed that this strong *S*-wave impedance contrast, not surprisingly, gave rise to a strong converted-wave or *P-S* reflection from the top of the reservoir.

Based on these modeling results, Chevron and partners acquired a 67 km^2 4-C/3-D survey of Alba Field which produced very striking results. The converted-wave or *P-S* data showed a greatly improved image of the reservoir as compared with the *P-P* image in almost every part of the field (Figure 9).

Attenuation of free-surface multiples. A number of interesting methods for attenuating free-surface multiples have been developed recently. Like the dual-sensor idea, these methods can be developed using *z* transform theory.

One of the most general methods is described by Berkhout and Verschuur (1997) and Weglein et al. (1997). Weglein gives a clear explanation of this method using

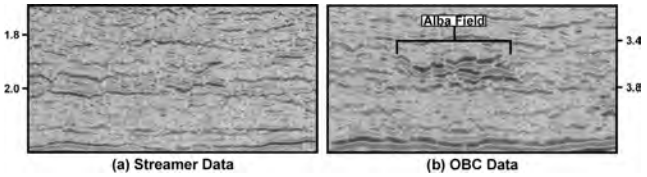

Figure 9. Comparison of (a) streamer and (b) converted-wave OBC data from Alba Field, North Sea. The converted-wave data provide a much clearer image of the reservoir interval (modified from MacLeod et al.).

inverse-scattering theory. The method can be understood by examining the free-surface reflections in terms of the upcoming wavefield as in equation (4). Instead of a single reflection R, consider $R(Z)$ as the z transform of the reflectivity sequence:

$$U(Z) = \frac{R(Z)}{[1 + R(Z)]} \tag{13}$$

In this equation, $U(Z)$ is equivalent to $R_f(Z)$ in Weglein (1999).

We can rewrite (13) in terms of a series in $U(Z)$

$$\begin{aligned} U(Z)[1 + R(Z)] &= R(Z) \\ R(Z)[1 - U(Z)] &= U(Z) \\ R(Z) &= \frac{U(Z)}{[1 - U(Z)]} \end{aligned} \tag{14}$$

Expanding the series given by equation (14), we arrive at:

$$\begin{aligned} R(Z) &= U(Z)[1 + U(Z) + U^2(Z) + ...] \\ &= U(Z) + U^2(Z) + U^3(Z) + ... \end{aligned} \tag{15}$$

It is interesting to note that the upcoming reflectivity series of primaries and internal multiples, $R(Z)$, can be expressed in terms of infinite series of the total upgoing wavefield in the presence of a free-surface, $U(Z)$.

Equation (15) states that the reflectivity sequence, R(Z), can be constructed by successive convolutions of the total wavefield with itself (i.e. $U(Z)$, $U^2(Z)$, $U^3(Z)$...). This extraction of reflectivity from the total wavefield can be achieved by surface recording (and without any subsurface model assumptions) with Weglein's inverse scattering approach. However, it does assume a stationary behavior to the multiple sequence.

A multiple suppression scheme which utilizes both surface and OBC recording is given by Ikelle (1999). The derivation of Ikelle's method can be obtained by recalling Weglein's analysis. In Weglein's inverse scattering analysis given by equation (14), the total reflectivity can be generated by adding higher-order terms in the recordings of the total wavefield.

Ikelle shows that a similar inverse scattering relationship holds for the OBC recording. If $D(Z)$ is the OBC wavefield and $U(Z)$ is the upgoing wavefield recorded at the surface, then $D(Z) = Z^{1/2}U(Z)$. That is, the OBC recording is a time-delayed version of the surface recording. Also, the upgoing compressions change to downgoing rarefractions at the free-surface, and vice-versa. For the geophones located in the ocean-bottom sensor, $D(Z) = Z^{1/2}U(Z)$ and for the hydrophone $D(Z) = -Z^{1/2}U(Z)$. Therefore, it is

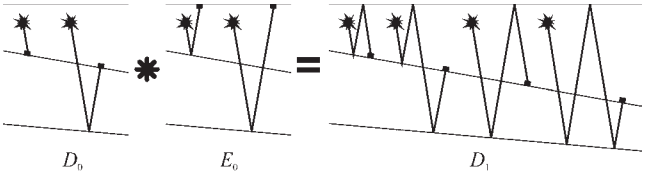

Figure 10. An example of combining streamer and OBC primaries to produce OBC multiples (modified from Ikelle, 1999).

not surprising that the inverse-scattering relationship given by Ikelle is similar to Weglein. That is,

$$D_p(Z) = D_0(Z) + D_1(Z) + D_2(Z)... \tag{16}$$

where $D_p(Z)$ is the reflectivity sequence expressed in terms of higher order multiple sequences. This is Ikelle's equation (1) without the source wavelet term (we consider the source wavelet deconvolution to be a separate problem). Ikelle shows that the OBC sequence of higher-order multiples (i.e., $D_1(Z)$, $D_2(Z)$,...) can be generated by combining both OBC and streamer data.

A simple example of Ikelle's relationship between the OBC and streamer recording is shown in Figure 10. Consider a water layer with one-way propagation time t_1 overlying a rock layer of one-way propagation time t_2. Using Ikelle's notation, the following arrivals in Figure 10 are defined:

D_0 = arrivals at OBC which are direct or primary reflection arrivals
E_0 = arrivals at streamer which are direct or primary reflection arrivals
D_1 = arrivals at OBC which are first-order receiver ghosts and first-order multiples.

The arrivals in D_0 are given by a downgoing compression of unit amplitude at time t_1 and an upgoing compression of amplitude R_2 at time $t_1 + 2t_2$. The z transform is:

$$D_0(z) = z^{t1} + R_2 z^{t_1 + 2t_2} \tag{17}$$

where Z used previously equals $z^{2t_1} = z^\tau$. Recall z relates to the sample interval and Z to the two-way time through the water layer.

The arrivals in E_0 are given by an upgoing compression of amplitude R_1 at time $2t_1$ and an upgoing compression of amplitude R_2 at time $2t_1 + 2t_2$. The z transform is:

$$E_0(z) = R_1 z^{2t_1} + R_2 z^{2t_1 + 2t_2} \tag{18}$$

The arrivals in D_1 are given by a downgoing rarefraction of amplitude R_1 at time $3t_1$, an upgoing rarefraction of amplitude R_1R_2 at time $3t_1 + 2t_2$, a downgoing rarefraction of amplitude R_2 at time $3t_1 + 2t_2$ and an upgoing rarefraction of amplitude R_2^2 at time $3t_1 + 4t_2$. The z transform is:

$$D_1(z) = -R_1 z^{3t_1} - R_1R_2 z^{3t_1 + 2t_2} - R_2 z^{3t_1 + 2t_2} - R_2^2 z^{3t_1 + 4t_2} \tag{19}$$

Therefore by comparing $D_0(z)E_0(z)$ to $D_1(z)$, we have:

$$\begin{aligned} D_0(z)E_0(z) &= (z^{t_1} + R_2 z^{t_1 + 2t_2})(R_1 z^{2t_1} + R_2 z^{2t_1 + 2t_2}) \\ &= R_1 z^{3t_1} + R_1R_2 z^{3t_1 + 2t_2} + R_2 z^{3t_1 + 2t_2} + R_2^2 z^{3t_1 + 4t_2} \\ &= -D_1(z) \end{aligned} \tag{20}$$

In other words, as equation (20) indicates, higher-order multiples measured at the OBC can be generated by using streamer data and lower-order multiples.

The use of the dual fields of displacement and pressure measured by ocean-bottom geophones and hydrophones to deconvolve multiples is analogous to handling of electric and magnetic fields in electromagnetism. For this reason, the use of dual fields is called Einstein deconvolution by Robinson (2000) in his discussion of dual-sensors.

Suggestions for further reading. "Attenuation of water-column reverberations using pressure and velocity detectors in a water-bottom cable" by Barr and Sanders (SEG 1989 *Expanded Abstracts*). "Estimation of multiple scattering by iterative inversion, Part I: Theoretical considerations" by Berkhourt and Verschuur (GEOPHYSICS, 1997). "Marine four-component seismic test, Gulf of Mexico: subsalt imaging at Mahogany Field" by Caldwell et al. (SEG 1998 *Expanded Abstracts*). "Ocean-bottom cable dual-sensor scaling" by Dragoset and Barr (SEG 1994 *Expanded Abstracts*). "Imaging through gas-filled sediments using marine shear-wave data" by Granli et al. (GEOPHYSICS, 1999). "Combining two seismic experiments to attenuate free-surface multiples in OBC data" by Ikelle (*Geophysical Prospecting*, 1999). "Deterministic estimation of a wavelet using impedance type technique" by Loewenthal et al. (*Geophysical Prospecting*, 1985). "On unified dual fields and Einstein deconvolution" by Robinson (GEOPHYSICS, 2000). "The Alba Field OBC seismic survey" by MacLeod et al. (EAGE 1999 *Expanded Abstracts*). "Removal of water-layer multiples from multicomponent sea-bottom data" by Osen et al. (GEOPHYSICS, 1999). "An improved method for determining water bottom reflectivities from dual-sensor ocean bottom cable data" by Paffenholz and Barr (SEG 1995 *Expanded Abstracts*). "Wavelet estimation and Einstein deconvolution" by Robinson (*TLE*, 2000). "How can the inverse-scattering method really predict and subtract all multiples from a multidimensional earth with absolutely no subsurface information?" by Weglein (*TLE* 1999). "An inverse scattering series method for attenuating multiples in seismic reflection data" by Weglein et al. (GEOPHYSICS, 1997). "Computed seismic speeds and attenuation in rocks with partial gas saturation" by White (GEOPHYSICS, 1975). TLE

Acknowledgments: We thank Larry Mewhort of Husky Oil Operations and Larry Sydora of Hibernia Management and Development Company for well information which aided in the construction of the general elastic-wave model of the Jeanne d'Arc Basin. We thank John Granli and Børge Arntsen of Statoil for seismic images of Tommeliten Field. Finally, we thank all sponsors of the CREWES Project for technical and financial support.

Corresponding author: bhoffe@geo.ucalgary.ca